Table VII. Comparison of Rate Constants for Hydrolysis and Aminolysis of Chelated and Free Glycine and β-Alanine Esters (25.0 °C)

	n = 1, mol^{-1} dm^3 s^{-1}	n = 2, mol^{-1} dm^3 s^{-1}	ref
$H_3N^+(CH_2)_nCO_2Et + H_2O$	1×10^{-10}	1×10^{-11}	*a,b*
$H_2N(CH_2)_nCO_2i\text{-}Pr + OH^-$	0.2	2×10^{-2}	*c,d*
$[Co(en)_2(H_2N(CH_2)_nCO_2i\text{-}Pr)]^{3+} + H_2O$	2.0×10^{-5}	8.3×10^{-7}	*e,f*
$[Co(en)_2(H_2N(CH_2)_nCO_2i\text{-}Pr)]^{3+} + OH^-$	1.5×10^{6}	4×10^{4}	*g,f*
$[Co(en)_2(H_2N(CH_2)_nCO_2i\text{-}Pr)]^{3+} + NH_2CH_2CO_2Et + OH^-$	4.7×10^{5}	3.9×10^{3}	*g,d*
$[Co(en)_2(H_2N(CH_2)_nCO_2i\text{-}Pr)]^{3+} + 2H_2NCH_2CO_2Et$	0.39	3.5×10^{-2}	*g,d*

[a] Conley, H. L.; Martin, R. B. *J. Chem. Phys.* **1965**, *69*, 2914. [b] Based on a factor of 10 slower for the β-alanine ester. [c] Hay, R. W.; Porter, L. J.; Morris, P. J. *Aust. J. Chem.* **1960**, *19*, 1197. A factor of 5 slower for R = *i*-Pr vs. Et. [d] This study. [e] Alexander, M. D.; Busch, D. H. *J. Am. Chem. Soc.* **1966**, *88*, 1130. [f] Reference 3. [g] Reference 1.

suggests that this may be due in part to greater relief of chelate ring strain on forming the addition intermediate in the five-membered system, facilitating addition, and in this regard the rate accelerations found for the β-alanine system are more likely to be applicable in the general case to monodentate esters.

It is now clear from this study and from the companion study on hydrolysis[3] that direct activation by the metal facilitates the addition of nucleophiles and retards elimination sufficient to require the formation of stable addition intermediates. Although this simple principle is the basis of all metal ion activation and has been recognized for many years,[9] previously only the addition part has been examined experimentally. A good example of this is in the metal-ion-catalyzed hydrolysis of nitriles[1] where only addition is involved. It is now clear that for esters (and the data for the hydrolysis of amides[11] can be similarly interpreted) that elimination is rate-controlling with good nucleophiles. Of more fundamental significance is the observation that the metal appears to stabilize the addition intermediate between transition states for addition and elimination. That is, a stepwise process is favored as opposed to a concerted reaction.[12] The reason for this is not entirely clear at the present time, but stabilization of such intermediates may well be largely entropic in nature.[3] For Co(III) overall rate accelerations vary from 10^4 to 10^6 depending on whether aminolysis or hydrolysis is involved. A further 10-fold increase is found for Ru(III) and Pt(IV), and first-row divalent transition metals are some 10^2 less effective.

Amine addition is not rate-determining because loss of $^+NH_2R$ from the intermediate is always favored over loss of RO^-. For the corresponding hydrolysis intermediate competitive loss of HO^- and RO^-

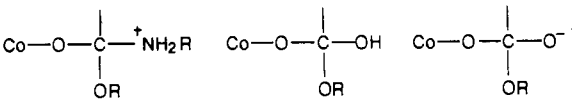

occurs with the order being $HO^- > MeO^- > EtO^- > i\text{-}PrO^-$.[3] Deprotonation of this intermediate accelerates loss of RO^- by $\sim 10^5$. General acids will affect in a similar way the departure of both leaving groups, and no general-acid catalysis has been observed in the reactions of these activated esters. For the amine–alcohol intermediate general-acid-catalyzed loss of ROH has not been observed in aqueous solution probably because the solvent provides this factor, but it has been observed in Me_2SO.[2]

Registry No. $[Co(en)_2(\beta\text{-alaO-}i\text{-Pr})](ClO_4)_3$, 103477-73-2; $[Co(en)_2(\beta\text{-ala-glyOEt})](ClO_4)_2(NO_3)$, 103477-75-4; β-alanine isopropyl ester, 39825-36-0; glycine ethyl ester, 459-73-4.

Supplementary Material Available: Rate data for the reactions of glycine ethyl ester (Table I), imidazole (Table IV), and glycine ethyl ester and imidazole (Table V) with $[Co(en)_2(\beta\text{-alaO-}i\text{-Pr})]^{3+}$ (4 pages). Ordering information is given on any current masthead page.

Contribution from the Department of Chemistry,
York University, North York, Ontario M3J 1P3, Canada

Equilibria for Phosphine Ligation to Ferrous Protoporphyrin IX Dimethyl Ester and Related Systems in Toluene[1]

Dennis V. Stynes,* David Fletcher, and Xuening Chen

Received April 19, 1986

Spectrophotometrically derived equilibrium constants for tributylphosphine (PBu_3) and tributyl phosphite ($P(OBu)_3$) binding to methylimidazole (MeIm) complexes of iron protoporphyrin IX dimethyl ester (Hm) are reported and compared with new and literature-derived values for ferrous phthalocyanine (FePc) and ferrous dimethylglyoxime ($Fe(DMGH)_2$) analogues. Affinities increase for all three systems in the order MeIm < $P(OBu)_3$ < PBu_3. Carbon monoxide binding and mutual trans destabilization of $P(OBu)_3$ increases in the order FePc < $Fe(DMGH)_2$ < Hm, consistent with axial π-donor ability of iron being greatest in hemes and least in FePc. New carbonyl derivatives of hemes with trans PR_3 have Soret bands at 440 nm. Trans to CO, MeIm is preferred to phosphine ligands. Rate constants for the heme systems estimated from equilibrium data and measured at low temperature are compared with those for FePc and $Fe(DMGH)_2$ analogues. Trends in K_{eq} are most easily understood in terms of rate constants for ligand dissociation, which provide a reliable indicator of coordinate bond energies. Trans effects in hemes and phthalocyanine complexes are similar but differ somewhat from previously established trends in bis(dioxime) complexes of iron.

Introduction

Axial ligand substitution reactions of low-spin six-coordinate hemes proceed via a dissociative mechanism with rates at 25 °C in the range 10^4–10^{-2} s^{-1}.[2-5] Equilibrium constants for ligation of imidazoles, carbon monoxide, etc. to a variety of hemes have also been obtained by spectrophotometric methods.[6-10] Extensive rate and equilibrium data are also available for non-heme FeN_4XY

(1) Abbreviations: Equilibrium constants $K^T_{X,Y}$ are for replacement of X by Y trans to T. Rate constants k^T_{-X} are for dissociation of X trans to T; k^T_{+X} is for addition of X trans to T. The shortened forms N (MeIm), P (PBu_3), and PO ($P(OBu)_3$) are used as subscripts and superscripts.
(2) Weschler, C. J.; Anderson, D. L.; Basolo, F. *J. Am. Chem. Soc.* **1975**, *97*, 6707.
(3) White, D. K.; Cannon, J. B.; Traylor, T. G. *J. Am. Chem. Soc.* **1979**, *101*, 2443.
(4) Lavalette, D.; Tetreau, C.; Momenteau, M. *J. Am. Chem. Soc.* **1979**, 101, 5395.
(5) Traylor, T. G.; Tsuchiya, S.; Campbell, D.; Mitchell, M.; Stynes, D. V.; Koga, N. *J. Am. Chem.* Soc. **1985**, *107*, 604.
(6) Brault, D.; Rougee, M. *Biochem. Biophys. Res. Commun.* **1974**, *57*, 654.
(7) Rougee, M.; Brault, D. *Biochemistry* **1975**, *14*, 4100.
(8) Wayland, B. B.; Mehne, L. F.; Swartz, J. *J. Am. Chem. Soc.* **1978**, *100*, 2379.
(9) Ellis, P. E.; Linard, J. E.; Symanski, T.; Jones, R. D.; Budge, J. R.; Basolo, F. *J. Am. Chem. Soc.* **1980**, *102*, 1889.
(10) Olson, J. S.; McKinnie, R. E.; Mims, M. P.; White, D. K. *J. Am. Chem. Soc.* **1983**, *105*, 1522.

0020-1669/86/1325-3483$01.50/0

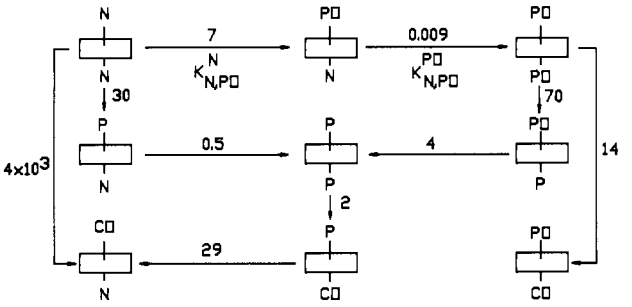

Figure 1. Reaction scheme. Equilibrium constants at 25 °C in toluene are given for the direction shown.

complexes, where N_4 is phthalocyanine[11-13] or bis(dioxime).[14,15]

Equilibrium constants for ligation to iron (eq 1–4) are related to corresponding on-rate (k_+) and off-rate (k_-) constants on the basis of the well-established dissociative mechanism. On-rate

$$HmX_2 \underset{k_{+X}}{\overset{k_{-X}}{\rightleftharpoons}} HmX \underset{k_{-Y}}{\overset{k_{+Y}}{\rightleftharpoons}} HmXY \qquad (1)$$

$$Hm + X \rightleftharpoons HmX \qquad K_X = k_{+X}/k_{-X} \qquad (2)$$

$$HmX + X \rightleftharpoons HmX_2 \qquad K^X_X = k^X_{+X}/k^X_{-X} \qquad (3)$$

$$HmX_2 + Y \rightleftharpoons HmXY + X$$
$$K^X_{X,Y} = (k^X_{+Y}/k^X_{+X})(k^X_{-X}/k^X_{-Y}) \qquad (4)$$

differences are typically small,[16] and therefore the equilibria are largely governed by the large effects on the off rates. The off-rate constants (or $\Delta H_{-X}^{\ddagger}$) are a good measure of the relative magnitude of coordinate bond energies. Differences in the binding constants in hemes and between hemes and other systems are most reliably interpreted in terms of these rate parameters.

A detailed study of rate in the dimethylglyoxime system[14] has led to a better understanding of the nature of the trans effects of σ-donor and π-acceptor ligands. A few phosphine derivatives of hemes[17] and hemoproteins[18,19] have been described. However, no mixed-π-acid derivatives have been previously reported. Herein we describe equilibrium and kinetic investigations of phosphine and new mixed-phosphine–carbonyl complexes of ferrous protoporphyrin IX dimethyl ester.

Experimental Section

The ligands MeIm, PBu_3, and $P(OBu)_3$ were Aldrich reagents. Solutions of hemes and PBu_3 were handled under nitrogen or argon. Hemin chloride (Sigma) was converted to the dimethyl ester by a literature method.[20] Toluene was distilled from $LiAlH_4$ and MeIm from KOH prior to use. $FePc(PBu_3)_2$ and $FePc(P(OBu)_3)_2$ were prepared as described by Sweigart.[13]

Equilibrium Determinations. A few microliters of a concentrated solution of hemin chloride in $CHCl_3$ was injected into 2 mL of toluene containing $\sim10^{-2}$ M ligand (L = PBu_3, $P(OBu)_3$, or MeIm) under argon and shaken with aqueous dithionite. The toluene solution of the reduced hemochrome was separated from the aqueous layer by cannulation under argon. Solutions for spectrophotometric measurements were obtained by injecting 10–50 μL of this hemochrome solution into ~3 mL of dry degassed toluene under nitrogen typically containing an excess of the appropriate ligand to give absorbances in 1-cm cuvettes of ~1 in the Soret region. Spectrophotometric titrations were carried out at 25 °C by standard methods and absorbance data analyzed by microcomputer. Spectra were obtained on a Aminco DW-2A or Hitachi-Perkin-Elmer 340 spectrophotometer.

Low-temperature kinetic measurements were made in a Pyrex Dewar cell of 2 cm path length. Temperatures were maintained by chlorobenzene (−45 °C) or carbon tetrachloride (−23 °C) slush baths. The dual-wavelength capability of an Aminco DW-2A spectrophotometer had to be used since our low-temperature cell blocks the reference beam for split-beam operation. Absorbance data at one or more wavelengths were analyzed as described previously.[14] Rates were independent of entering ligand concentrations (typically 0.1 M or greater) in all cases studied.

Table I. Soret Bands (λ_{max}, nm) for Hemes HmXY at 25 °C in Toluene

	Y			
X	MeIm	PBu_3	$P(OBu)_3$	BzNC
MeIm	428			
PBu_3	437	458		
$P(OBu)_3$	433	456	449	
BzNC	429	448	442	435
CO	420	440	432	

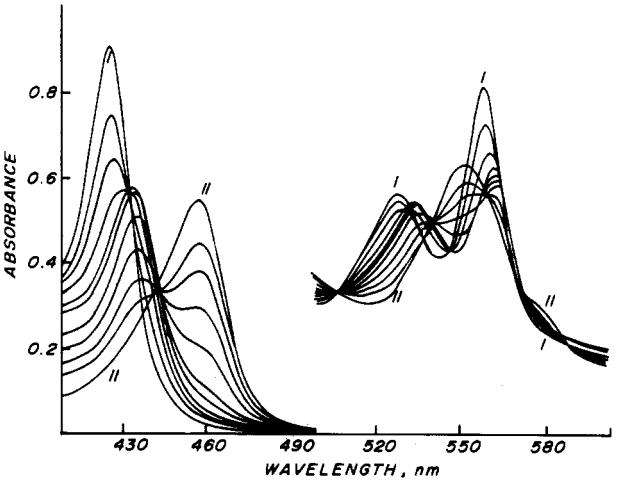

Figure 2. Spectrophotometric data for titration of $Hm(MeIm)_2$ with PBu_3. Data are for 25 °C in toluene at fixed [MeIm] = 8.3×10^{-3} M and variable [PBu_3]. For spectra 1–11 [PBu_3] ($\times10^{-2}$ M) = 0, 0.013, 0.026, 0.052, 0.144, 0.25, 0.80, 1.7, 3.0, 29, and 180. The absorbance scale is expanded ×5 for the region 500–650 nm.

Results

Hemes. Equilibria. The overall binding scheme for equilibria investigated in this study is shown in Figure 1. The position of the Soret bands for the complexes studied is given in Table I. The Soret bands for the $Hm(PR_3)_2$ species are similar to those of previously reported spectra for FeTPP derivatives.[17] Most of the mixed-ligand species are new.

Phosphine Complexes. Addition of PR_3 (R = Bu or OBu) to solutions of $Hm(MeIm)_2$ containing excess MeIm results in two distinct sets of spectral changes as a function of [PR_3]. Typical data for PBu_3 shown in Figure 2 were analyzed in terms of the two successive binding constants $K^N_{N,P}$ and $K^P_{N,P}$. The $Hm(MeIm)(PBu_3)$ species λ_{max} = 437 nm makes up ~80% of spectrum 5 in Figure 2. The corresponding titration with $P(OBu)_3$ gives an even larger separation of the successive equilibria $K^N_{N,PO}$ and $K^{PO}_{N,PO}$, allowing accurate determination of both constants.

Titration of $Hm(P(OBu)_3)_2$ with PBu_3 also resulted in two distinct sets of spectral changes assigned to the equilibria $K^{PO}_{PO,P}$ and $K^P_{PO,P}$. In this case the middle species $Hm(P(OBu)_3)(PBu_3)$ has an extinction coefficient at 454 nm which is greater than that of either $Hm(PBu_3)_2$ or $Hm(P(OBu_3))_2$. This results in an increase in absorbance during titration of $K^{PO}_{PO,P}$ and a decrease during titration of $K^P_{PO,P}$. The ratio [$P(OBu)_3$]/[PBu_3] at which the absorbance at 454 nm is a maximum is equal to

(11) Stynes, D. V.; James, B. R. *J. Am. Chem. Soc.* **1974**, *96*, 2733.
(12) Stynes, D. V. *Inorg. Chem.* **1977**, *16*, 1170.
(13) Martinsen, J.; Miller, M.; Trojan, D.; Sweigart, D. A. *Inorg. Chem.* **1980**, *19*, 2162.
(14) Chen, X.; Stynes, D. V. *Inorg. Chem.* **1986**, *25*, 1173.
(15) Siddiqui, N.; Stynes, D. V. *Inorg. Chem.* **1986**, *25*, 1982.
(16) For cases with no steric effects, on-rate constants for imidazoles, isocyanides, and CO are typically in the range 10^7–10^8 M^{-1} s^{-1} at 25 °C.[3,4] Small differences in on-rate in hemes and other FeN_4 systems are discussed elsewhere.[14]
(17) Ohya, T.; Morohoshi, H.; Sato, M. *Inorg. Chem.* **1984**, *23*, 1303.
(18) Sono, M.; Dawson, J. H.; Hager, L. P. *Inorg. Chem.* **1985**, *24*, 4339.
(19) Dawson, J. H.; Andersson, L. A.; Sono, M. *J. Biol. Chem.* **1983**, *258*, 13637.
(20) Traylor, T. G.; Chang, C. K.; Geibel, J.; Berzinis, A.; Mincey, T.; Cannon, J. *J. Am. Chem. Soc.* **1979**, *101*, 6716.

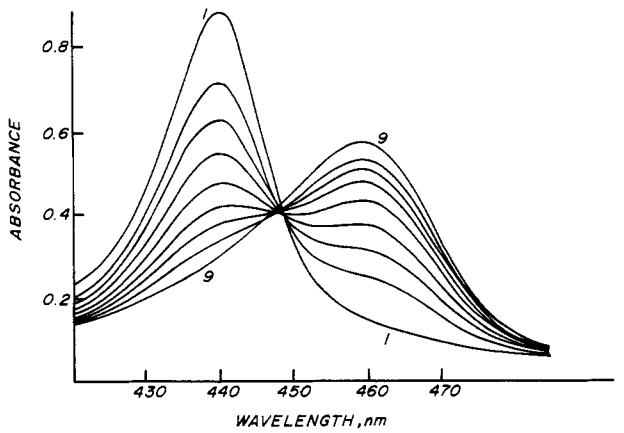

Figure 3. Spectrophotometric data for titration of $Hm(PBu_3)(CO)$ with PBu_3. Data are at 25 °C in CO-saturated toluene with $[PBu_3]$ ($\times 10^{-2}$ M) = 0.1, 0.5, 0.9, 1.6, 2.8, 4.8, 8.1, and 19 in spectra 1–8, respectively. Spectrum 9 occurs after CO is purged with argon.

Table II. Equilibrium Constants for $FeN_4TL + E \rightleftharpoons FeN_4TE + L$

$K^T_{L,E}$	heme[a]	FePc	$Fe(DMGH)_2$[c]
$K^N{}_{N,P}$	30	50[b]	98
$K^P{}_{N,P}$	0.5	2.6[a]	5
$K^N{}_{N,PO}$	7	9[b]	19
$K^{PO}{}_{N,PO}$	0.009	0.16[b]	0.10
$K^{PO}{}_{PO,P}$	70	23[a]	77
$K^P{}_{PO,P}$	4	6[a]	5
$K^P{}_{P,CO}$	1.7[e]	g	0.023
$K^{PO}{}_{PO,CO}$	14	$\sim 10^{-4}$ [a,g]	0.066
$K^{CO}{}_{P,N}$	29[e]		11
$K^N{}_{N,CO}$	7×10^3 [d]	0.03[f]	123

[a] At 25 °C in toluene; this work. [b] Calculated from rate data from ref 13; in acetone solution at 21 °C. [c] Calculated from rate data at 60 °C from ref 14. [d] For deuteroheme.[7] [e] From least-squares fit of K_{app} vs. $[PBu_3]$ for $[PBu_3]$ ($\times 10^{-3}$ M) = 1.3, 6.7, 13, 26; K_{app} = 27, 18, 14, and 9, respectively. From is defined in eq 7. [f] Reference 11. [g] Binding is too weak for an accurate determination.

$(K^{PO}{}_{PO,P}K^P{}_{PO,P})^{1/2}$. The product $K^{PO}{}_{PO,P}K^P{}_{PO,P} = 280 \pm 60$ obtained by this method is in good agreement with the quotient of equilibrium constants calculated from eq 5. Only small absorbance changes were observed in titration of $K^P{}_{PO,P}$ at high values of $[PBu_3]$. Therefore, the most accurate estimate for this constant was obtained by using the overall constant $K_{overall} = K^{PO}{}_{PO,P}K^P{}_{PO,P}$ obtained as above and the value of $K^{PO}{}_{PO,P}$ obtained from the titration data at lower $[PBu_3]$ at λ = 458 nm, where a large absorbance change is observed primarily associated with $K^{PO}{}_{PO,P}$.

$$K^{PO}{}_{PO,P}K^P{}_{PO,P} = \frac{K^N{}_{N,P}K^P{}_{N,P}}{K^N{}_{N,PO}K^{PO}{}_{N,PO}} = 240 \pm 50 \qquad (5)$$

CO Binding. Toluene solutions of $Hm(PR_3)_2$ undergo spectral changes in the presence of CO (see Figure 3) assigned to the equilibrium

$$Hm(PR_3)_2 + CO \rightleftharpoons Hm(PR_3)(CO) + PR_3 \qquad (6)$$

Equilibrium constants were obtained by titration at fixed [CO] (1 atm) and variable $[PR_3]$. A $Hm(H_2O)(CO)$ species (λ_{max} = 414 nm) analogous to that reported for a tetraphenylporphyrin system[6] was not a problem if dry toluene was used and at least 10^{-3} M excess PR_3 was present. Data are given in Table II.

Titrations of $Hm(PBu_3)(CO)$ at 1 atm CO and 1.3×10^{-3} M PBu_3 with MeIm shown in Figure 4 afforded clean isosbestic points consistent with formation of only Hm(MeIm)(CO). Under the conditions used $Hm(MeIm)_2$ and $Hm(MeIm)(PBu_3)$ are negligible; however, a small amount of $Hm(PBu_3)_2$ is present. Spectrophotometric data for titrations of solutions containing equilibrium mixtures of $Hm(PBu_3)(CO)$ and $Hm(PBu_3)_2$ at higher

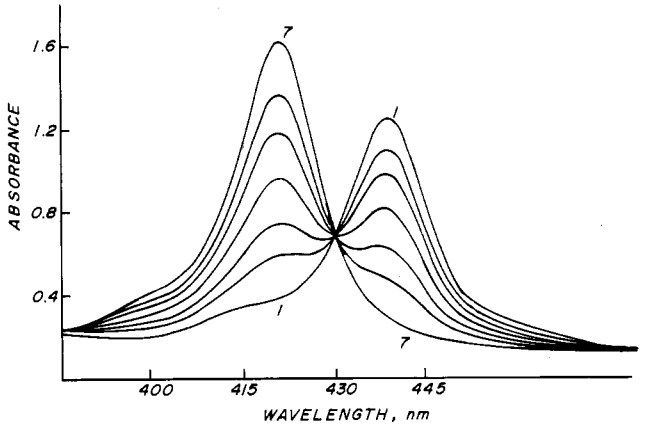

Figure 4. Spectrophotometric data for titration of an equilibrium mixture of $Hm(PBu_3)_2$ and $Hm(PBu_3)(CO)$ with MeIm. Data are at 25 °C in CO-saturated toluene at fixed $[PBu_3] = 1.3 \times 10^{-3}$ M variable [MeIm]. For spectra 1–7 [MeIm] (10^{-3} M) 0, 0.011, 0.022, 0.044, 0.088, 0.17, and 4.0 M respectively.

$[PBu_3]$ containing as much as 70% $Hm(PBu_3)_2$ were analyzed to give the apparent equilibrium constant K_{App}

$$K_{App} = \frac{A - A_0}{A_\infty - A}\frac{[PBu_3]}{[MeIm]} \qquad (7)$$

where A_0 is the absorbance of the equilibrated mixture of $Hm(PBu_3)_2$ and $Hm(PBu_3)(CO)$ and A_∞ is the absorbance at high [MeIm] where only Hm(MeIm)(CO) is present. It can be shown that K_{App} is related to the separate equilibria $K^P{}_{P,CO}$ and $K^{CO}{}_{P,N}$ by eq 8. A linear plot of $1/K_{App}$ vs. $[PBu_3]$ for experiments at fixed [CO] gives $K_{P,CO} = 1.7$. A least-squares analysis of data given in footnote *e* of Table II is in good agreement with that obtained from the direct titration of the equilibrium $K^P{}_{P,CO}$.

$$K_{App} = K^{CO}{}_{P,N}/\left(1 + K^P{}_{P,CO}{}^{-1}\frac{[PBu_3]}{[CO]}\right) \qquad (8)$$

Kinetics. The reactions of $Hm(MeIm)_2$ with PR_3 are complete on mixing at 25 °C. The rates can be obtained as previously described for some reactions[2] of FeTPP systems at −45 °C. Addition of excess PBu_3 (>0.1 M) to a solution of $Hm(MeIm)_2$ results in only slight buildup of $Hm(MeIm)(PBu_3)$ and a first-order decrease in absorbance at 428 nm ($Hm(MeIm)_2$) with a corresponding increase at 458 nm ($Hm(PBu_3)_2$) (k = 0.025 s^{-1}) indicative of a slow $k^N{}_{-N}$ followed by a more rapid $k^P{}_{-N}$:

$$Hm(MeIm)_2 \underset{k^N{}_{-P}}{\overset{k^N{}_{-N}}{\rightleftharpoons}} Hm(MeIm)(PBu_3) \underset{k^P{}_{-P}}{\overset{k^P{}_{-N}}{\rightleftharpoons}} Hm(PBu_3)_2 \qquad (9)$$

If one starts with a solution of $Hm(MeIm)(PBu_3)$ generated in situ from $Hm(PBu_3)_2$ and 10^{-3} M MeIm (containing negligible $Hm(MeIm)_2$), addition of excess PBu_3 results in a clean first-order reaction affording $k^P{}_{-N} = 0.06$ s^{-1} at −45 °C.

The corresponding experiments with $P(OBu)_3$ proceed similarly, giving $k^N{}_{-N} = 0.025$ s^{-1} and $k^{PO}{}_{-N} = 0.055$ s^{-1}.

The reaction of $Hm(PBu_3)_2$ with MeIm at low temperatures (the reverse of eq 9) proceeds in two distinct steps, first giving the product $Hm(PBu_3)(MeIm)$, λ_{max} = 437 nm, at the rate $k^P{}_{-P}$ = 0.014 s^{-1} at −45 °C. The subsequent slower reaction to give $Hm(MeIm)_2$, λ_{max} = 428 nm, was more conveniently studied at −23 °C, giving the rate constant $k^N{}_{-P} = 1 \times 10^{-3}$ s^{-1}.

The corresponding reaction of $Hm(P(OBu)_3)_2$ at −45 °C gives $Hm(MeIm)(P(OBu)_3)$ (λ_{max} = 433 nm) complete on mixing followed by a slower second step, $k^N{}_{-PO} = 2.5 \times 10^{-3}$ s^{-1}, giving $Hm(MeIm)_2$ (λ_{max} = 428 nm).

The $Hm(PBu_3)(CO)$ complex, λ_{max} = 440 nm, reacted with excess PBu_3

$$Hm(PBu_3)(CO) + PBu_3 \xrightarrow{k^P{}_{-CO}} Hm(PBu_3)_2 + CO \qquad (10)$$

at −45 °C at the pseudo-first-order rate $k = 0.06$ s^{-1}. The cor-

Table III. Kinetic Data for Dissociation of Ligand L Trans to T in HmLT Complexes in Toluene (k^{T}_{-L}, s^{-1})[a]

		T				
L	temp, °C	MeIm	PBu_3	$P(OBu)_3$	BzNC	CO
MeIm	25	15[f,h]				2.6[c]
	−23					2.4×10^{-3}
	−45	0.025	0.060	0.055	0.01	8×10^{-5}
PBu_3	25	13[f]				20[f]
	−23	1×10^{-3}			2.0×10^{-3}	
	−45		0.014		1.5×10^{-4}	
$P(OBu)_3$	25	54[f]				1000[f]
	−45	2.5×10^{-3}		>0.1	0.038	
BzNC	25	0.5[e]				
	0	9.6×10^{-3}				
	−23				8.3×10^{-3}	
	−45		$>2 \times 10^{-4}$		2.0×10^{-4}	
CO	25	0.02[d]				6×10^{4}[f]
	−45	$\sim 10^{-6}$	0.06	>0.1		

[a] This work. [b] FeTPP.[4] [c] FeDHD(Im).[3] [d] Chelated protoheme.[5] [e] Chelated protoheme.[10] [f] Calculated from equilibrium constants as described in text.

responding $Hm(P(OBu)_3)(CO)$ complex reacted too rapidly even at −45 °C with excess $P(OBu)_3$ to obtain the rate k^{PO}_{-CO}.

Reaction of $Hm(BzNC)_2$, λ_{max} = 435 nm, with PBu_3 at −45 °C proceeds directly to give $Hm(PBu_3)_2$, λ_{max} = 458 nm, $k = 2 \times 10^{-4}$ s^{-1}, with clean isosbestic points

$$Hm(BzNC)_2 \xrightarrow[\text{slow}]{k^{BzNC}_{-BzNC}} Hm(BzNC)(PBu_3) \xrightarrow[\text{fast}]{k^{P}_{-BzNC}} Hm(PBu_3)_2 \quad (11)$$

indicating that $k^{BzNC}_{-BzNC} < k^{P}_{-BzNC}$. The corresponding reaction with MeIm gives a two-step reaction also affording k^{BzNC}_{-BzNC} and k^{N}_{-BzNC}:

$$Hm(BzNC)_2 \xrightarrow[\text{slow}]{k^{BzNC}_{-BzNC}} Hm(BzNC)(MeIm) \xrightarrow[\text{slower}]{k^{N}_{-BzNC}} Hm(MeIm)_2 \quad (12)$$

The reverses of reactions 11 nd 12 were also investigated. Reaction of $Hm(PBu_3)_2$ with excess BzNC at −45 °C gives a rapid reaction with formation of $Hm(PBu_3)(BzNC)$ at a rate k^{P}_{-P} (identical with that obtained in the reaction with MeIm) followed by a slower clean first-order reaction to give $Hm(BzNC)_2$. Reaction of $Hm(MeIm)_2$ with BzNC at −45 °C gave two consecutive first-order rates; the first k^{N}_{-N} results in small absorbance changes while the second gives a large increase in absorbance at 436 nm, where $Hm(BzNC)_2$ absorbs, from which k^{BzNC}_{-N} is obtained. These results establish the trans-effect orders for MeIm, PBu_3, $P(OBu)_3$, and BzNC. Kinetic data are collected in Table III.

For Hm(MeIm)(CO) the MeIm is more labile than CO, thus allowing direct determination of k^{CO}_{-N}. Addition of PBu_3 at low temperatures results in formation of $Hm(PBu_3)_2$, λ_{max} = 458 nm, via eq 13 with clean isosbestics and no evidence for the inter-

$$Hm(MeIm)(CO) \xrightarrow{k^{CO}_{-N}} Hm(PBu_3)(CO) \xrightarrow{\text{fast}} Hm(PBu_3)_2 \quad (13)$$

mediate species $Hm(PBu_3)(CO)$, known to absorb at 440 nm. The first step is rate-determining. The alternative path involving initial CO loss is negligibly slow at this temperature. Rate constants at −23 and −45 °C are given in Table III. Corresponding rates for PBu_3 and $P(OBu)_3$ dissociation trans to CO could not be obtained since, in both cases, the reaction goes via eq 14, where

$$Hm(PBu_3)(CO) + MeIm \xrightarrow{\text{fast}} Hm(PBu_3)(MeIm) \xrightarrow{\text{slow}} Hm(MeIm)_2 \quad (14)$$

the CO is replaced in the rate-determining step. The experiment clearly shows that $k^{CO}_{-P} < k^{P}_{-CO}$ since, if the PBu_3 were replaced first, the very inert (at −45 °C) Hm(MeIm)(CO) would be produced with a characteristic spectrum easily distinguished from that of the observed product.

Table IV. Kinetic Data for FePcTL Complexes (k^{T}_{-L}, 10^3 s^{-1})

	T			
L	MeIm	PBu_3[d]	$P(OBu)_3$[b]	BzNC[a]
MeIm	1.5[a]	150 (2 °C)	2300	14
PBu_3	1.8[d] (50 °C)	1 (−23 °C)		
$P(OBu)_3$	0.1[b,c]		50 000	
RNC	0.035[a]			200

[a] In Toluene at 25 °C. [b] Acetone at 21 °C.[13] [c] Trans ligand is imidazole. [d] In toluene; this work.

FePc. Several relevant kinetic and equilibrium constants for phosphine ligation in FePc have been previously reported by Sweigart (in acetone at 21 °C).

We have determined the following equilibria starting from $FePc(PR_3)_2$ in toluene since all three are kinetically labile at 25 °C. (Formation of $FePc(MeIm)_2$ is sufficiently slow that no significant amount of this species forms during the determination.)

$$FePc(P(OBu)_3)_2 + PBu_3 \rightleftharpoons FePc(P(OBu)_3)(PBu_3) + P(OBu)_3 \quad (15)$$

$$FePc(P(OBu)_3)(PBu_3) + PBu_3 \rightleftharpoons FePc(PBu_3)_2 + P(OBu)_3 \quad (16)$$

$$FePc(PR_3)(MeIm) + PR_3 \rightleftharpoons FePc(PR_3)_2 + MeIm \quad (17)$$

The $FePc(P(OBu)_3)(PBu_3)$ complex is isosbestic with $FePc(PBu_3)_2$ at λ = 437 nm, where $FePc(P(OBu)_3)_2$ has a maximum, allowing a straightforward determination of $K^{PO}_{PO,P}$. This result was then used in a two-equilibrium analysis of absorbance data at three other wavelengths, 470, 410, and 370 nm, where large absorbance changes are observed for both steps.

Spectral changes assigned to CO binding to $FePc(PBu_3)_2$ could only be observed in CO-saturated toluene at very high dilution (<10^{-6} M FePc):

$$FePc(PBu_3)_2 + CO \rightleftharpoons FePc(PBu_3)(CO) + PBu_3 \quad (18)$$

A very rough estimate of $K^{P}_{P,CO} = 10^{-4}$ could be made on the basis of the decrease in absorbance at 437 nm in the presence of CO. Equilibrium constants for the kinetically more inert complexes have been calculated from kinetic data. These data are collected in Table II. Rates were determined for the following reactions in toluene solution:

$$FePc(PBu_3)_2 + MeIm \underset{k^{P}_{-N}}{\overset{k_{-P}}{\rightleftharpoons}} FePc(MeIm)(PBu_3) \xrightleftharpoons{k^{N}_{-P}} FePc(MeIm)_2 \quad (19)$$

Addition of excess MeIm to a solution of $FePc(PBu_3)_2$ gives the $FePc(MeIm)(PBu_3)$ species on mixing at 25 °C with a decrease

at 468 nm. This reaction could be followed at −23 °C. The second step to give the $FePc(MeIm)_2$ species is very slow and was studied at 50 °C. The reverse reaction of the $FePc(MeIm)(PR_3)$ complex with excess PBu_3 was obtained at 2 °C. These data are collected in Table IV along with the relevant literature data.

$Fe(DMGH)_2$. All of the relevant equilibria in this system are kinetically slow to equilibrate. Therefore, we have calculated equilibria at 60 °C using the extensive kinetic data and eq 4 previously described.[14] In some cases, assumptions regarding competitive on-rates have been made, but in most cases, these values have been determined by kinetic methods as described previously. The different temperature used for these data does not significantly alter the comparisons made.

Discussion

The equilibrium constants for ligand subsitution in Table II summarize the thermodynamic differences between the different FeN_4 systems heme, FePc, and $Fe(DMGH)_2$. A number of similarities exist. For all K's except those involving CO binding, the trends in the three systems are quite similar. The relative affinity order PBu_3 > $P(OBu)_3$ > MeIm trans to MeIm is identical in all three systems.

The CO binding constants show the greatest differences, heme > DMGH > Pc, as previously discussed for the trans ligand MeIm.[11] The $K^X_{X,CO}$ value decreases substantially when X is also a good π acceptor in all three systems, and from $K^{CO}_{P,N}$ one sees that, trans to CO, MeIm is preferred to PBu_3 while the opposite is the case trans to N ($K^N_{N,P}$). These effects may be qualitatively understood in terms of the synergistic nature of CO binding and the competition of two π acceptors in trans positions.

Trans Effects. The low-temperature kinetic studies described in the previous section clearly establish the trans-effect order for hemes, and this order is different from that found in $Fe(DMGH)_2$ and FePc. In $Fe(DMGH)_2$ the general trans-effect order MeIm > PBu_3 > $P(OBu_3)$ > BzNC ≥ CO was observed for all leaving groups except the strongest π acceptor CO.[14] In FePc the trans-effect order is uniformly $PBu_3 \approx P(OBu)_3$ > BzNC > MeIm for loss of MeIm, PBu_3, or $P(OBu)_3$.

In hemes, Table III clearly shows the trans-effect order.

$PBu_3 \geq P(OBu)_3$ > MeIm > BzNC > CO for loss of MeIm, and for the data shown, this order is essentially the same for loss of PBu_3 or $P(OBu)_3$.

For loss of the strong π acceptor CO, the trans effects CO > $P(OBu)_3 \approx PBu_3$ >> MeIm are similar for hemes and $Fe(DMGH)_2$. Binding of CO to FePc is too weak to obtain data trans to π-acceptor ligands; however, a similar trend is apparent.

The following generalizations can be made:

1. Strong π acceptors like CO delabilize trans σ donors because of a synergistic bonding interaction.
2. Weaker π acceptors show a similar but smaller effect in all three FeN_4 systems.
3. Strong π acceptors mutually labilize each other in trans positions.
4. Methylimidazole generally shows different trans effects in $Fe(DMGH)_2$ vs. FePc or Hm systems.

While the Hm and FePc systems both give an approximately similar trans-effect order for loss of MeIm, the magnitudes of the effects are dramatically different. In Hm, k_{-N} spans only a factor of 6 for MeIm, PBu_3, $P(OBu)_3$, and BzNC and only CO truly has a large trans effect. In FePc, MeIm and PBu_3 differ by 10^3 and BzNC is labilizing relative to MeIm in FePc but somewhat delabilizing in Hm. We believe these differences reflect differences in the relative importance of σ and π bonding in these systems. Stronger in-plane π interactions in FePc would lead to a greater synergistic cis stabilization by MeIm than in Hm.

This effect has also been shown in BQDH vs. DMGH complexes, where a systematic variation of π interactions is possible.[15] Here one observes the position of MeIm in the trans-effect series moves to become less labilizing than PBu_3 as the in-plane π interaction increases. While it was only possible to obtain k^{CO}_{-X} for X = MeIm, the corresponding values for X = PBu_3, $P(OBu)_3$, and CO can be estimated,[21] with use of eq 4, from equilibrium constants from this work and those reported for other systems if one assumes k_{+CO} is independent of the trans ligand and the ratio $k_{+X}/k_{+CO} = 4$. These values are included in Table III and indicate CO has a trans effect similar to that of MeIm for k_{-P} but becomes quite labilizing relative to MeIm for k_{-PO} and k_{-CO} due to $\pi-\pi$ interactions.

Values of k^N_{-X} may also be calculated from equilibria and eq 4 if assumptions are made about k_{+N}/k_{+X}. We have used the rate constant k^N_{-N} for FeTPP at 25 °C and assumed $k_{+N}/k_{+X} = 4$ (as for $Fe(DMGH)_2$)[15] to obtain approximate estimates for k^N_{-X} at 25 °C. These estimates are not inconsistent with the low-temperature data but could be in error by a factor of 2 because of the approximations used.

Coordination Bond Energies. We believe the rate constants for ligand dissociation and the trans effects in different systems provide the most logical basis for interpreting the binding constants. In most cases, it is important to make a clear distinction between kinetics and thermodynamics. However, for these systems, the fundamental rate constants for metal–ligand bond breaking, k_{-L}, provide an excellent measure of coordinate bond energy differences and these bond energies are precisely the information required to interpret the equilibrium data in a meaningful way. Rigorously, a coordinate bond energy for ligand X in FeN_4XY is the heat of the gas-phase reaction

$$FeN_4XY \rightarrow FeN_4Y + X \qquad (20)$$

This is closely approximated by the solution-phase (toluene) energy ΔH^* for k_{-X}.[22] This coordinate bond energy is not transferable to FeN_4XZ since large trans effects are typical in these systems. Furthermore, one must recognize that the "bond energy" is not localized in the Fe–X bond. Much of the Fe–X bond energy could reside in changes in FeN_4 or FeY bonds in the hexa- and pentacoordinate species. There is no unambiguous way of dividing the net axial bond energy between X and Y. For example, the overall thermodynamic stability of Hm(MeIm)(CO) is given by the sum of free energies or product of K's. $K_{overall} \sim 10^{12}$ for successive addition of the two axial ligands:[23]

$$Hm + CO \underset{}{\overset{\sim 10^4}{\rightleftharpoons}} Hm(CO) \overset{\sim 10^8}{\rightleftharpoons} Hm(MeIm)(CO) \qquad (21)$$

$$Hm + MeIm \overset{\sim 10^4}{\rightleftharpoons} Hm(MeIm) \overset{\sim 10^8}{\rightleftharpoons} Hm(MeIm)(CO) \qquad (22)$$

If we add CO first, we infer a much stronger Hm–N bond, but reversing the order, we would infer a much stronger Hm–CO bond. Only the sum of all bond energies in a complex is defined, and there is no thermodynamic basis for defining separate bond energies, except arbitrarily. Kinetic data provide a rational basis for dividing up the bond energies in these complexes and understanding why bond energies change from one molecule to another.

It is reasonable to suggest that the stronger bond is the one most difficult to break in a molecule. On the basis of this definition

$$Hm(CO) \overset{k^{CO}_{-N}}{\longleftarrow} Hm(MeIm)(CO) \overset{k^N_{-CO}}{\longrightarrow} Hm(MeIm) \qquad (23)$$

we see that the Hm–CO bond is stronger than the Hm–MeIm bond in Hm(MeIm)(CO). If we wish to compare the Hm–X bonds in this molecule with Hm–X bonds in other molecules, we

(21) Successive equilibria for CO binding to FeTPP are $K_{CO} = 6.6 \times 10^4$ and $K^{CO}_{CO} = 190\ M^{-1}$ at 25 °C in benzene.[8] The corresponding values for FeDHD are 5×10^4 and $210\ M^{-1}$, respectively.[7] The FeDHD system is considered more appropriate for comparison with Hm. Assumptions regarding on-rates are justified elsewhere.[14]

(22) ΔH^* differs from $\Delta H°$ by the enthalpy of activation for addition to the pentacoordinate complex, ΔH^*_{+X}. By the principle of microscopic reversibility the on-rate barrier includes solvation/reorganization effects as well as differences between a severely stretched (ΔH^*_{-X}) vs. severed metal–ligand bond ($\Delta H°$). These are typically small and, on the basis of trends in k_{+X}, do not vary greatly as a function of the ligand. Since ΔS^*_{-X} values are also very similar,[14,15] one is justified in general using k_{-X} as a qualitative measure of bond strengths.

(23) Specific values of K depend slightly on the porphyrin (TPP vs. DHD), but the orders of magnitudes shown are valid for all hemes.

Table V. Comparison of Kinetic and Equilibrium Data for CO Binding[a]

$$FeN_4(MeIm)_2 + CO \rightleftharpoons FeN_4(MeIm)(CO) + MeIm$$

	heme	FePc	$Fe(DMGH)_2$	$Fe(BQDH)_2$ (10 °C)
$K^N{}_{N,CO}$	7×10^3 [a]	0.03	125	~3
k_{+N}/k_{+CO}	17	4	8	
$k^N{}_{-N}$, s^{-1}	1500	1.5×10^{-3}	5.2×10^{-3}	$\sim 6 \times 10^{-2}$
$k^N{}_{-CO}$, s^{-1}	0.02	0.02	10^{-6}	2×10^{-3}
ν_{CO}, cm^{-1}	1970	1995	1978	2028

[a] Collected from previous tables and published data for hemes,[3-5] FePc,[11] $Fe(DMGH)_2$,[14] and $Fe(BQDH)_2$.[15] All data are at 25 °C in toluene. The heme data are for various porphyrins and are only approximately self-consistent.

Table VI. Comparison of Kinetic and Equilibrium Data for $P(OBu)_3$ Binding[a]

$$Fe(MeIm)_2 \overset{K^N{}_{N,PO}}{\rightleftharpoons} Fe(MeIm)(P(OBu)_3) \overset{K^{PO}{}_{N,PO}}{\rightleftharpoons} Fe(P(OBu)_3)_2$$

	Hm (25, −45 °C)[b]	Pc (25 °C)	DMGH (60 °C)	BQDH (10 °C)
$K^N{}_{N,PO}$	7	9	19	50
$K^{PO}{}_{N,PO}$	0.009	0.16	0.1	1
K_1/K_2	780	56	190	50
$k^N{}_{-N}$	0.02	0.0015	0.5	0.06
$k^{PO}{}_{-N}$	0.05	2.3	5.7×10^{-4}	2.2×10^{-3}
$k^N{}_{-PO}$	2.5×10^{-3}	10^{-4}	7×10^{-3}	3×10^{-4}
$k^{PO}{}_{-PO}$	>0.1	50	1.5×10^{-3}	5.3×10^{-4}

[a] Collected from previous tables and published data for FePc,[11-13] $Fe(DMGH)_2$,[14] and $Fe(BQDH)_2$.[15] Some of the FePc data are for 21 °C in acetone;[13] the rest are for toluene solution. [b] Equilibrium constants at 25 °C, rate constants at −45 °C.

can then describe "effects". For example, the Hm–N bond is clearly stronger in Hm(MeIm)(CO) than in either Hm(MeIm) or $Hm(MeIm)_2$. The ligand CO has the effect of strengthening the Hm–N bond (note that this does not require that the Hm–N bond be shorter)[24] since much of the added strength of the Hm–N bond may actually reside in the Hm–CO bond. The rate constants k_{-N} and k_{-CO} provide a measure of these effects, which allow a more rational interpretation of equilibria.

Table V summarizes data pertinent to the equilibrium

$$FeN_4(MeIm)_2 + CO \rightleftharpoons FeN_4(MeIm)(CO) + MeIm \quad (24)$$

The overall equilibrium constants span 10^5; however, it is incorrect to claim that CO binds more strongly to hemes than FePc on the basis of the data. The individual rate constants clearly show that Hm and FePc differ in their affinities for MeIm (10^6), and in fact k_{-CO} shows that their CO binding is the same. The correlation of K with ν_{CO} then is a coincidence.

For the closely related oxime systems, the difference between DMGH and BQDH is found primarily in k_{-CO} and here one is justified in claiming a difference in CO binding which correlates with ν_{CO}.

In Table VI data relevant to the successive binding constants for $P(OBu)_3$ are collected. While the ratios $K^N{}_{N,PO}/K^{PO}{}_{N,PO}$ differ only slightly in the four systems, the trans effects that give rise to them are dramatically different.

The separate equilibria may be expressed in terms of the rate parameters (eq 25), and the ratio then (after on-rate parameters are cancelled out) depends upon two factors: the trans effect of MeIm vs. $P(OBu)_3$ on loss of MeIm and that on loss of $P(OBu)_3$.

$$K^N{}_{N,PO} = \frac{k^N{}_{-N}}{k^N{}_{-PO}} \frac{k_{+PO}}{k_{+N}} \qquad K^{PO}{}_{N,PO} = \frac{k^{PO}{}_{-N}}{k^{PO}{}_{-PO}} \frac{k_{+PO}}{k_{+N}} \quad (25)$$

The approximate contributions of these two factors are shown in eq 26.

$$\frac{K^N{}_{N,PO}}{K^{PO}{}_{N,PO}} = \frac{k^N{}_{-N}}{k^{PO}{}_{-N}} \frac{k^{PO}{}_{-PO}}{k^N{}_{-PO}} \quad (26)$$

heme	$780 \approx 0.4 \times \sim 10^3$
Pc	$56 \approx (6 \times 10^{-4}) \times (5 \times 10^4)$
DMGH	$190 \approx 900 \times 0.2$
BQDH	$50 \approx 27 \times 1.7$

The heme system is dominated by the trans effect of $P(OBu)_3$ due to π–π destabilization. In FePc, the small ratio disguises the two large effects that are present. Here $P(OBu)_3$ is strongly labilizing relative to MeIm for both MeIm and $P(OBu)_3$.

In $Fe(DMGH)_2$ the greater trans-stabilizing effect of $P(OBu)_3$ on MeIm vs. that of $P(OBu)_3$ is important. Note that in this system both MeIm and $P(OBu)_3$ are more inert trans to $P(OBu)_3$ but the effect is much larger on MeIm. For the BQDH system, where axial π interactions are less important, the trans-effect differences on MeIm and $P(OBu)_3$ are smaller.

The overall pattern that emerges from this analysis is that ligation to FeN_4 systems follows systematic trends. Hemes have inherently weaker axial bonding than the other systems, which makes them substantially more labile as six-coordinate complexes and also allows detection of lower coordination number species.

Large differences between FeN_4XY systems can arise from the different way in which cis and trans effects operate as a result of the extensive bonding interactions between N_4, X, and Y. These differences become apparent if kinetic data are available.

Acknowledgment. D.F. is an NSERC Undergraduate Scholar. Support of the Natural Sciences and Engineering Research Council is gratefully acknowledged.

Registry No. (Hm)(MeIm)(PBu_3), 103712-28-3; (Hm)(MeIm)($P(OBu)_3$), 103712-29-4; (Hm)(PBu_3)$_2$, 103712-30-7; (Hm)($P(OBu)_3$)(PBu_3), 103712-31-8; (Hm)($P(OBu)_3$)$_2$, 103712-32-9; (Hm)(BzNC)(MeIm), 103712-33-0; (Hm)(BzNC)(PBu_3), 103712-34-1; (Hm)(BzNC)($P(OBu)_3$), 103712-35-2; (Hm)(BzNC)$_2$, 103712-36-3; (Hm)(CO)(MeIm), 58450-69-4; (Hm)(CO)(PBu_3), 103712-37-4; (Hm)(CO)($P(OBu)_3$), 103712-38-5; FePc($P(OBu)_3$)$_2$, 61005-31-0; FePc($P(OBu)_3$)(PBu_3), 73612-18-7; FePc(PBu_3)(MeIm), 103712-39-6; FePc(PBu_3)$_2$, 61005-30-9; $Fe(DMGH)_2$, 15665-27-7; MeIm, 30346-87-3; PBu_3, 998-40-3; $P(OBu)_3$, 102-85-2; BzNC, 10340-91-7; CO, 630-08-0.

(24) Structural data show the Fe–N bonds are about 0.1 Å longer trans to CO vs. trans to MeIm: Peng, S.; Ibers, J. A. *J. Am. Chem. Soc.* **1976**, *98*, 8032.